Electronic structure and properties of AlN

Eliseo Ruiz and Santiago Alvarez
Departament de Química Inorgànica, Universitat de Barcelona, Diagonal 647, 08028 Barcelona, Spain

Pere Alemany
Departament de Química Física, Universitat de Barcelona, Diagonal 647, 08028 Barcelona, Spain
(Received 17 November 1993)

The electronic structure of the wurtzite-type phase of aluminum nitride has been investigated by means of periodic *ab initio* Hartree-Fock calculations. The binding energy, lattice parameters (a,c), and the internal coordinate (u) have been calculated. All structural parameters are in excellent agreement with the experimental data. The electronic structure and bonding in AlN are analyzed by means of density-of-states projections and electron-density maps. The calculated values of the bulk modulus, its pressure derivative, the optical-phonon frequencies at the center of the Brillouin zone, and the full set of elastic constants are in good agreement with the experimental data.

INTRODUCTION

Aluminum nitride is a tetrahedrally coordinated III-V compound which crystallizes at ambient conditions in the hexagonal wurtzite structure.[1] This structure differs from the cubic zinc-blende one adopted by some of the III-V compounds mainly in the relative positions of the third neighbors and beyond. AlN has a large band gap (about 6.3 eV),[2] a high thermal conductivity (up to 320 W/mK),[3,4] and a small thermal-expansion coefficient.[5] These properties make this material an attractive candidate for applications as a ceramic substrate in thin-film devices. Because of its piezoelectric properties it has also been used in thin-film microwave acoustic resonator applications.[6]

Although single crystals of AlN are not easily grown, measurements of several physical properties for this compound have been reported. The valence charge density, determined from precise x-ray-diffraction experiments,[7] suggests that the bonding is highly ionic. Nevertheless, the adoption of the tetrahedrally coordinated wurtzite structure by the compound at ambient conditions rather than the rocksalt one, indicates that some degree of covalency is present. This is also consistent with the fracture toughness exhibited by AlN, which may be related to its partially covalent nature. Spectroscopic studies including Raman,[8–13] infrared,[9] reflectivity, and transmission spectra,[14] x-ray photoemission spectroscopy (XPS),[2] ultraviolet photoemission spectroscopy (UPS),[15] electron-energy-loss spectroscopy (EELS),[16] and Auger spectra[16] have been reported for AlN. The material constants, i.e., elastic stiffness, piezoelectricity, and permitivity, also have been calculated from measured surface acoustic wave phase velocities[17] and Brillouin spectra.[11]

Several band-structure calculations have been reported for AlN using different methods. The earlier studies were performed by Hejda and Hauptmanová,[18] using the orthogonalized plane-wave (OPW) method, by Bloom[19] with the empirical pseudopotential method, by Kobayashi *et al.*[20] with a semiempirical tight-binding calculation, and by Huang and Ching[21] with the semi-*ab initio* linear combination of atomic orbitals (LCAO) method. More recently, different *ab initio* approaches have been used in the study of the electronic structure of AlN. Ching and Harmon[22] performed orthogonalized linear combination of atomic orbitals (OLCAO) calculations in the local-density approximation. The same method also has been used for the evaluation of optical properties for this material.[23] Recently, Miwa and Fukumoto reported a local-density functional study of the structural, electronic, and vibrational properties of GaN and AlN. There has also been great interest in the calculation of high-pressure properties of aluminum nitride.[24] Several papers reported electronic structure calculations for the wurtzite and other cubic phases (rocksalt and zinc blende) of AlN.[25–29]

The calculations presented in this paper were largely motivated by the aim of testing the performance of the periodic Hartree-Fock method in the calculation of some properties (bulk modulus, elastic constants, and phonon frequencies) for a system with noncubic symmetry. Special attention is paid to the ability of different basis sets to reproduce the experimental data.

METHODOLOGY

The calculations reported in the present work were performed using the CRYSTAL-92 program,[30] which provides self-consistent solutions to the Hartree-Fock-Roothan equations subject to periodic boundary conditions. Details of the mathematical formulation of this method have been previously described,[31] and will be omitted here.

CRYSTAL-92 uses linear combinations of Gaussian orbitals to construct a localized atomic basis from which Bloch functions are built up. As in the molecular Hartree-Fock calculations, the results can be quite sensitive to the choice of the basis set. Previous work using this methodology has shown that the standard basis sets used in molecular calculations must be modified for their

TABLE I. Optimized exponents for the most diffuse Gaussian functions used in the present calculations.

Basis set	α_{sp} (Al)	α_d (Al)	α_{sp} (N)	α_d (N)
6-21G	0.17		0.26	
6-21G^*	0.15	0.51	0.28	0.80
PS-21G	0.14		0.24	
PS-21G^*	0.14	0.39	0.26	0.78

use on periodic systems.[31] The program can work at the all-electron (AE) level as well as with effective core pseudopotentials (PS). In this paper we test four different basis sets. The 6-21G is an all-electron basis set with split-valence functions. Addition of d-type polarization functions on both atoms gives the 6-21G^* basis set. We also will examine the performance of two equivalent basis sets, PS-21G and PS-21G^*, which replace the core electrons by effective core pseudopotentials. Parameters for the Gaussian functions used in our work have been obtained from previous calculations for related systems by reoptimization of the exponents of the most diffuse functions using the experimental crystal structure.[32] Results of this reoptimization procedure are shown in Table I.

It is interesting to note here that in periodic Hartree-Fock calculations the number of bielectronic integrals to be evaluated, and therefore the computational cost of the calculation, strongly depends on the exponents of the more diffuse Gaussian functions included in the basis set. Hence it is sometimes possible to use all-electron basis sets with a lower computational cost than pseudopotential basis sets of the same quality. This paradoxical situation is found when comparing the time needed for calculations with the 6-21G^* and the PS-21G^* basis sets. The smaller exponents for the pseudopotential basis functions, especially on the polarization function of aluminum, make this basis set more expensive than the all-electron one.

Computational parameters controlling the truncation of both the Coulomb and exchange infinite series have been chosen to give a "good" level of accuracy defined in the sense of Pisani, Dovesi, and Roetti.[31]

RESULTS

Crystal structure. The wurtzite structure (Fig. 1) is hexagonal, $P6_3mc$ (num. 186) space group, with both types of atoms located at Fig. 2(b) positions.[1] A total of three parameters (a, c, and the internal coordinate u for one of the atoms) are needed to fully describe the structure. Table II shows results obtained from optimization of these three values with different basis sets.

The internal coordinate u has been obtained by evaluating the total energy as a function of u, keeping a and c at their optimum values. The curves were fitted to third-order polynomials with the minima indicated in Table II. For the "ideal" wurtzite structure a c/a ratio of 1.633 and an internal coordinate of 0.375 are expected.[33] Deviation from this value for the case of AlN indicates that the coordination of each atom is a distorted tetrahedron with three equal bonds forming aluminum-nitrogen layers parallel to the ab planes, and a fourth slightly longer bond in the c direction.

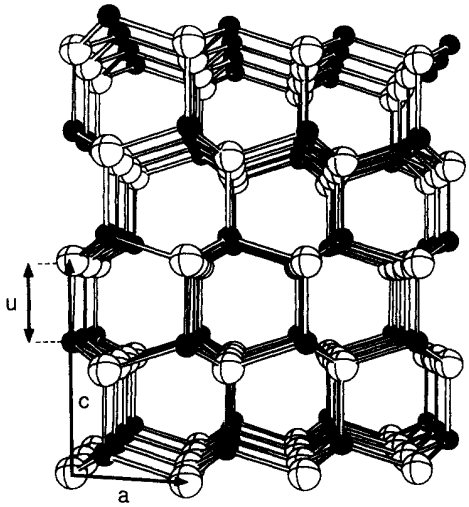

FIG. 1. Wurtzite-type structure of AlN. Black balls represent aluminum atoms, white ones nitrogen atoms.

From these data it is clear that the use of polarization functions both in the AE and PS cases results in a contraction of the structure, giving parameters closer to experimental ones. This observation agrees well with previ-

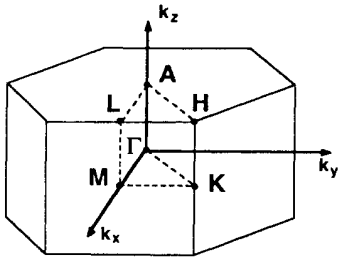

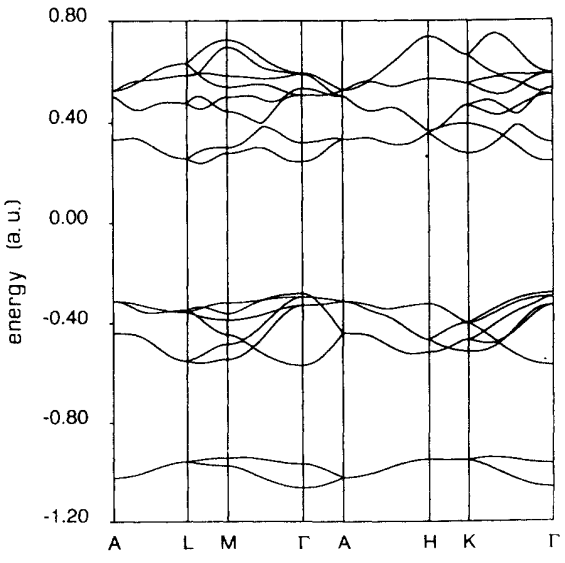

FIG. 2. Electronic band structure obtained with the 6-21G^* basis set for wurtzite-type AlN.

TABLE II. Structural properties calculated with the different basis sets used. Experimental data are provided for comparison. Distances are indicated for the two different bonds of the structure. $d_{Al\text{-}N}$ refers to the three equivalent Al-N bonds while $d'_{Al\text{-}N}$ is the distance for the unique bond in the c direction.

	6-21G	6-21G^*	PS-21G	PS-21G^*	Expt.
a (Å)	3.135	3.117	3.123	3.101	3.110[a]
c (Å)	4.986	4.982	4.988	4.975	4.980[a]
u	0.3832	0.3828	0.3822	0.3817	0.3821[a]
c/a	1.590	1.598	1.597	1.604	1.601
$d_{Al\text{-}N}$ (Å)	1.901	1.891	1.896	1.885	1.889
$d'_{Al\text{-}N}$ (Å)	1.911	1.909	1.906	1.899	1.903
BE (eV)	11.03	10.11	10.43	11.09	11.6[b]

[a]Reference 1.
[b]Reference 34.

ously published results, which show that addition of polarization functions always yields a reduction of lattice parameters as large as 1.5% when second-row elements are involved.[32]

Binding energies (BE's) reported in Table II are obtained as the difference between total energies of the bulk and the isolated atoms calculated with the same basis set. All calculated values are smaller than the experimental ones by about 4–13 %. This magnitude is well known always to be underestimated by the Hartree-Fock method, a problem that can be partly solved by an *a posteriori* inclusion of correlation contributions using density functionals of the correlation energy.[32]

Inclusion of polarization functions in the basis set usually leads to larger binding energies, as can be seen when comparing results for the two pseudopotential basis sets. For the all-electron basis sets the opposite trend is found. In this case the change of the optimized exponent of the sp orbitals in the valence shell of aluminum atoms ($\alpha_{sp}=0.17$ for 6-21G, and $\alpha_{sp}=0.15$ for 6-21G^*) has a larger influence on the calculated binding energy than the inclusion of polarization functions. The lower exponent in the 6-21G^* basis set results in a stabilization of both the isolated atom and the solid, although the improvement is much larger for the former, yielding a lower binding energy.

Band structure and density of states. The calculated band structure of AlN is presented in Fig. 2. These results show the existence of a direct band gap of 14.36 eV at the center of the Brillouin zone (Γ). This value is in strong disagreement with the experimental value of 6.6 eV determined by x-ray spectroscopy,[2] reflecting a well-known failure of the Hartree-Fock method, which overestimates this property. Except for the value of the band gap, our calculated band structure agrees well both in topology and in its main features with those previously published.[20–23] The calculated width of the valence band (8.27 eV) agrees well with the estimation of approximately 9 eV obtained from x-ray spectra.[2]

Figure 3 shows different projections of the AlN density of states. The valence band is split into two subbands. The lowest one is formed by the 2s levels of the nitrogen atoms. The main contribution to the top of the valence band comes from the 2p levels of nitrogen, while the bottom of the conduction band arises from the hybridization of the aluminum s and p orbitals. As can be seen from the projections, the contribution of the d-type polarization functions to the valence band is negligible, while their participation in the conduction band is more important, especially for aluminum atoms.

A comparison of calculated DOS and spectroscopic data is shown in Fig. 4. The UPS (Refs. 15 and 35) and x-ray emission spectra[2] obtained for the valence band of AlN are in good agreement with the calculated density of states (DOS). The width of this band is approximately 9 eV (0.33 a.u.) for the calculated DOS, coincident with that found in both types of spectra. The DOS curve and the spectra also agree in shape, both showing two main peaks. The conduction band has been studied by Fomi-

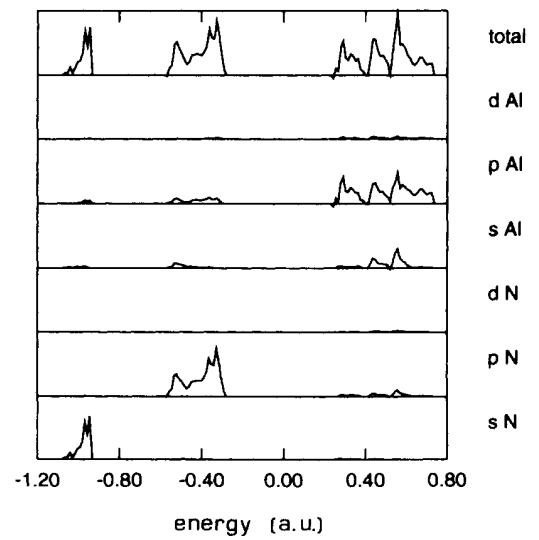

FIG. 3. Atomic orbital projections of the density of states obtained with the 6-21G^* basis set for the wurtzite phase of AlN. The atomic orbital contributions have been obtained using a Mulliken partition scheme.

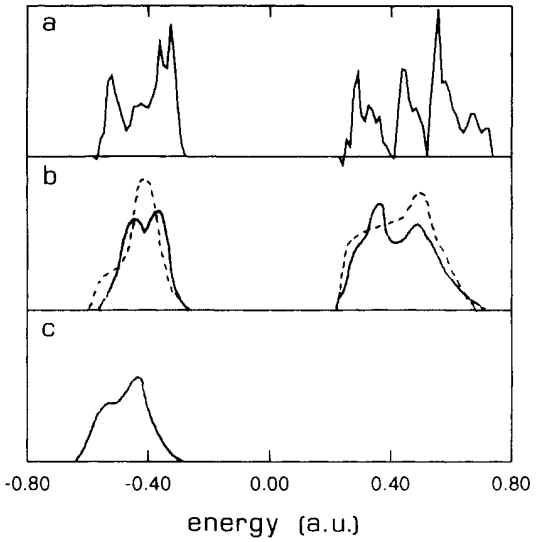

FIG 4. Comparison of the calculated DOS (a) with experimental x-ray emission spectra (b), and UPS spectra (c). The solid lines in (b) correspond to the Al spectra, the dashed ones to the N spectra. The x-ray emission spectra of the conduction band are shifted relative to those of the valence band in order to allow a better comparison with the calculated DOS. Intensities of the spectra are in arbitrary units.

chev[2] by measuring the spectral dependence of the quantum yield of the external photo effect of x-rays.[36] In this case the bandwidth of approximately 12 eV (0.44 a.u.) is also in good agreement with the calculated DOS. Both experimental and calculated data show three main peaks in this region.

Electron-density maps. The electron-density map obtained with the 6-21G^* basis set is reported in Fig. 5(a), whereas Fig. 5(b) shows the difference between the crystalline charge density and the superposition of the spherical atomic densities. Complementary information is supplied in Table III, where Mulliken population data are reported. As noted in earlier work, when dealing with periodic systems these values should be used in an even more qualitative way than for molecules.

Figure 5(a) shows a slight departure from spherical

TABLE III. Mulliken population data for the optimized structures with each of the basis sets employed. $q(A)$ is the Mulliken net charge of atom A (in electrons). Occupations for all valence orbitals are also listed. Distances and overlap populations are indicated for the two different bonds of the structure. $d_{\text{Al-N}}$ refers to the three equivalent Al-N bonds, while $d'_{\text{Al-N}}$ is the distance for the unique bond in the c direction.

	6-21G	6-21G^*	PS-21G	PS-21G^*
q (Al)	+1.934	+1.451	+2.086	+1.353
3s	0.414	0.502	0.369	0.458
3p	0.224	0.307	0.182	0.303
3d		0.029		0.055
q (N)	−1.934	−1.451	−2.086	−1.353
2s	1.883	1.778	1.910	1.730
2p	1.684	1.557	1.726	1.540
3d		0.001		0.000
$d_{\text{Al-N}}$ (Å)	1.901	1.981	1.896	1.885
ov. pop.	0.155	0.230	0.140	0.258
$d'_{\text{Al-N}}$ (Å)	1.911	1.909	1.906	1.899
ov. pop.	0.149	0.222	0.134	0.249

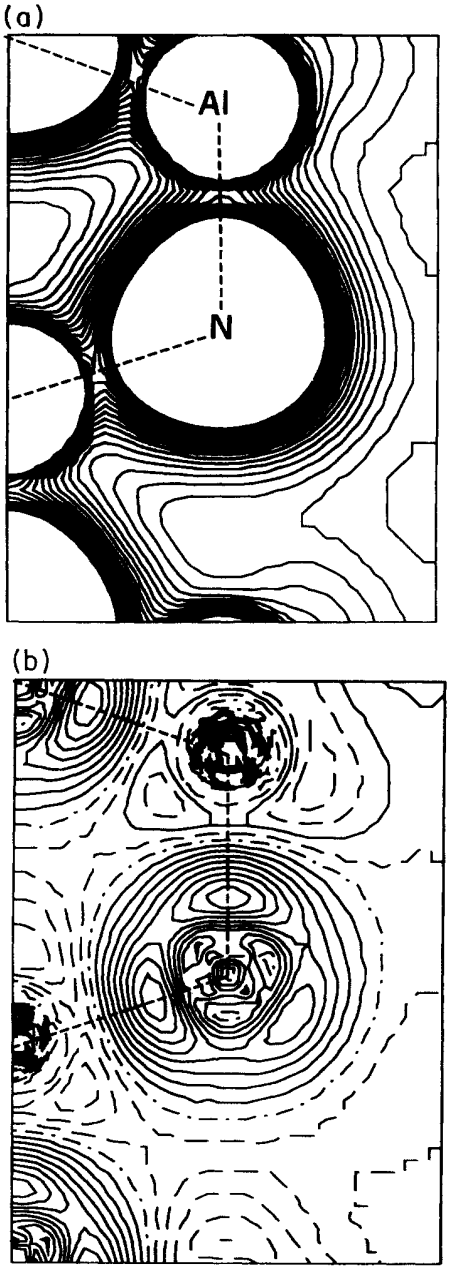

FIG. 5. Electron charge-density maps obtained with the 6-21G^* basis set for the wurtzite phase of AlN on a (11$\bar{2}$0) plane. (a) Total electron density. (b) Electronic charge difference between the studied system and the corresponding spherical atomic density superposition arrays. Values corresponding to neighboring isodensity lines differ by 0.01 e/bohr^3. The full and broken curves in (b) indicate density increase and decrease, respectively.

symmetry for the electronic density around nitrogen atoms. This distortion, with the electron density buildup located preferentially in the Al-N bonding regions [see Fig. 5(b)] arises from covalent contributions to the bonds in this compound. The electron-density maps are similar to those obtained for hexagonal wurtzite-type SiC,[37] although in SiC the greater covalent character results in a more pronounced departure from sphericity of the atomic electron clouds. The Mulliken population analysis (Table III) shows that in AlN the aluminum atoms act as cations, and the nitrogen atoms as anions. As a result, in the electron-density maps the distortion from spherical symmetry is almost unnoticeable for aluminum due to the lower polarizability of the cationic species. A difference map between the total electron density calculated with the 6-21G^* and the 6-21G basis sets (not shown in the figure) indicates that the effect of polarization functions is an accumulation of charge density in the Al-N bonding regions. Calculated electron-density maps are in good agreement with the experimentally determined ones.[7]

Mulliken population values presented in Table III clearly show that inclusion of polarization functions in the basis set results in a strong reduction of the ionicity of the structure, as can be observed in the atomic net charges and in the increase of the overlap populations for both types of Al-N bonds. This effect is due not only to the population of the polarization functions, but also to significant changes in the occupation of the s and p valence orbitals of both atom types. From the orbital occupations one can confirm that inclusion of polarization functions is more relevant for aluminum than for nitrogen.

Structure factors. In order to evaluate the quality of the electron charge density determined above, the structure factors associated with the 23 reflections explored by Sirota, Olekhnovich, and Olekhnovich[38] were calculated using the 6-21G^* basis set. Our results, which do not include vibrational effects on the structure factors, agree well with the values given by these authors at 0 K (Table IV).

In the refinement process of the x-ray experimental data, structure factors are usually determined by a least-squares procedure involving the "calculated" F's, obtained from a superposition of atomic charge distributions. The agreement coefficient defined as

$$R=\frac{\sum_i |F_i^{\rm exp}-F_i^{\rm calc}|}{\sum_i F_i^{\rm exp}}$$

is one of the indices used to estimate the quality of the fitting. Large values for R usually indicate a poor quality of the experimental data but could also arise from the inadequacy of the atomic superposition model. Typical experimental R values are of the order of 0.03. The R value obtained by comparing the structure factors calculated from the 6-21G^* electron density and the experimental data[38] is 0.02, indicating excellent agreement between the calculated and experimental charge densities.

Optical-phonon frequencies. A factor-group analysis may be used to predict the number and symmetry of the optical vibrations at the center of the Brillouin zone ($\mathbf{k}=\mathbf{0}$).[39,40] Accordingly, for space group $P6_3mc$, with two formula units per primitive cell, the irreducible representation for the optical phonons may be written as

$$\Gamma_{\rm op}=A_1+2B_1+E_1+2E_2 \ .$$

A_1, E_1, and E_2 are Raman active. A_1 and E_1 are also infrared active, and split into their longitudinal and transverse components (LO and TO). $B1$ is forbidden both in Raman and infrared.

In the present work we have used the so-called frozen phonon method[41,42] to evaluate the optical vibration frequencies at the center of the Brillouin zone for AlN. These frequencies are obtained from the evaluation of the total energy of the solid as a function of the movement of the atoms from their equilibrium positions according to the symmetry of each mode (see Fig. 6). For each optical mode the energy has been calculated at displacements from the equilibrium geometry of ± 0.0125, ± 0.025, and ± 0.050 Å. The vibration frequency is then evaluated from the second derivative of a second-order polynomial least-squares fit of these data. In our calculations, the longitudinal vibration frequencies cannot be obtained since they have contributions of the macroscopic electric field. Although a supercell method[42,43] has been proposed to overcome this limitation, it is computationally impractical in this system.

Table V shows the experimental and calculated optical-phonon frequencies for AlN. The calculated frequencies are in good agreement with most of the experimental data for the A_1, E_1, and E_2 modes. However, there is clear disagreement with the values reported by

TABLE IV. Static structure factors for AlN. Experimental values are from Ref. 38. Theoretical structure factors were calculated from the 6-21G^* electron density.

hkl	$F^{\rm expt}$	$F^{\rm calc}$
010	14.74	14.25
002	21.74	21.48
011	10.92	10.65
012	9.30	9.22
110	21.21	21.14
013	15.74	15.58
020	9.47	9.64
112	15.25	15.35
021	9.46	9.13
004	9.17	9.23
022	7.04	6.97
014	4.31	4.43
023	12.64	12.44
120	7.77	7.77
121	7.75	7.47
114	7.54	7.40
122	5.86	5.94
015	12.07	12.32
024	3.53	3.38
030	13.78	13.93
123	10.60	10.76
032	10.47	10.08
006	8.93	8.10

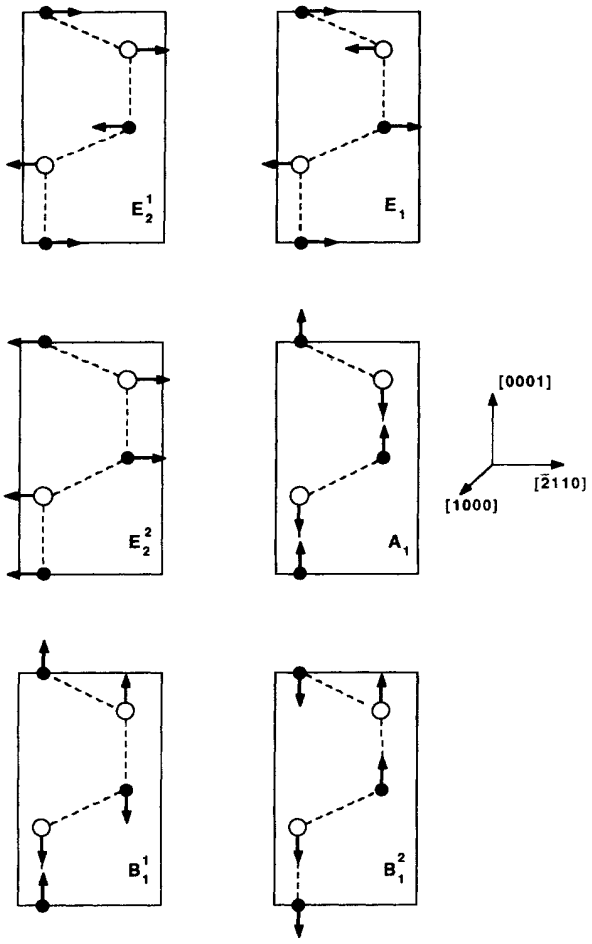

FIG. 6. Displacement vectors for the six optical phonons of the wurtzite structure.

Carlone, Lakin, and Shanks[9] for the A_1 and one of the E_2 modes. These authors have established a pattern for the frequency distribution of the wurtzites, and the E_2 modes of AlN seem not to fit well in it (see Fig. 5 in Ref. 9). Considering this regular pattern, in which our calculated frequency for the higher E_2 mode would fit perfectly, we are left to the conclusion that there is probably an ambiguity in the assignment of Carlone, Lakin, and Shanks.[9]

Let us finally note that all six optical modes have been treated as independent oscillators in our calculations. This approximation is strictly valid only for the A_1 and E_1 modes. The two modes with E_2 and those of B_1 symmetry are not independent, and each pair of vibrations belonging to the same symmetry species should be treated as coupled oscillators. The approximation of independent oscillators is probably reasonable for the E_2 modes, for which the mixing should be small due to the large frequency separation. This is not the case for the B_1 modes, for which important coupling might be expected. Although it is possible to solve this problem by the procedure developed by Kunc and Martin,[42] the lack of experimental information for comparison with calculated frequencies makes its application uninteresting.

Elastic properties. For each of the four basis sets, the total energy of the crystal has been evaluated for nine different volumes, keeping the c/a ratio fixed at the optimum value found for each case. From a third-order least-squares polynomial fit of these data, one can derive the equilibrium volume, the bulk modulus, and its pressure derivative (Table VI). As will be seen below, the bulk modulus also can be obtained from the calculated elastic constants. Comparison of the calculated values for the bulk modulus with those determined experimentally is not straightforward because of the high dispersion

TABLE V. Experimental and calculated AlN optical-phonon frequencies (in cm^{-1}) calculated with the 6-21G^* basis set at the center of the Brillouin zone.

Mode	Carlone[a]	Sanjurjo[b]	Collins[c]	Brafman[d]	Hayashi[e]	Perlin[f]	McNeil[g]	Calc.
A_1 (LO)	663	888	916	910			893	899[h]
A_1 (TO)		659	668	667	660	607	614	668
E_1 (LO)	821	895		910	910	924	916	989[h]
E_1 (TO)	614	671		667	672		673	734
$E_2^{(1)}$	303					241	252	301
$E_2^{(2)}$	426			665		660	660	704
$B_1^{(1)}$								723
$B_1^{(2)}$								772

[a]Reference 9.
[b]Reference 10.
[c]Reference 14.
[d]Reference 8.
[e]Reference 12.
[f]Reference 13.
[g]Reference 11.
[h]Estimated using the Lyddane-Sachs-Teller relation with $\varepsilon_0 = 8.50$ and $\varepsilon_\infty = 4.68$ from Ref. 54.

TABLE VI. Volume (V), bulk modulus (B), and its pressure derivative (B') calculated for AlN with different basis sets.

	6-21G	6-21G^*	PS-21G	PS-21G^*	Expt.
V (Å^3)	42.444	41.919	42.131	41.431	41.714[a]
B (GPa)	243	239	237	239	202[b], 208[c] 237[d], 160[e]
B'	4.45	3.77	4.30	4.19	6.3[c], 5.2[e]

[a]Reference 1.
[b]Reference 17.
[c]Reference 44.
[d]Reference 11.
[e]Reference 50.

in the measured results. Our calculated value is in good agreement with the higher experimental data. The calculated pressure derivative of the bulk modulus is underestimated with all four basis sets. A similar result is found when comparing the experimental values with other calculations based on the local-density approximation.[44]

Recent papers have described a straightforward method for the evaluation of the elastic constants of ionic crystals from Hartree-Fock calculations.[45–47] The total electron energy is evaluated point by point for several suitable unit-cell geometries (lattice strain) and different atomic fractional coordinates (inner strain). The elastic constants are then computed as second derivatives of the energy with respect to the different strain components. Data calculated by the present approach ignore all vibrational contributions to the energy, and thus should be compared to experimental values at 0 K corrected for the effect of zero-point vibrations.[46,48,49] When plotting measured elastic constants against temperature a slight linear increase is generally observed as T decreases. Calculated elastic constants are thus expected to be somewhat larger than experimental ones.

In the present work we have employed this approach for the evaluation of the five independent components of the elasticity tensor of the wurtzite phase of AlN. Elastic constants have been calculated numerically as second derivatives of the total crystal energy with respect to strain components ε_i, according to a second-order expansion of the elastic energy of the type

$$E=\tfrac{1}{2}\sum_{i,j=1}^{6} C_{ij}\varepsilon_i\varepsilon_j ,$$

where the Voigt contraction of subscripts for tensorial components is used.[51] Suitable lattice deformations $D=[\varepsilon_1\varepsilon_2\varepsilon_3\varepsilon_4\varepsilon_5\varepsilon_6]$ with all nonzero components equal were considered in order to express the energy E as a parabolic function of a single strain parameter (η). The coefficient in this function represents a linear combination of elastic constants C_{ij}. The five deformations employed are $D_1=[\eta 00000]$, $D_2=[\eta\eta 0000]$, $D_3=[\eta 0\eta 000]$, $D_4=[00\eta 000]$, and $D_5=[000\eta 00]$. Application of these deformations to the crystal structure of AlN gives five sets of energy data as a function of the strain parameter from which C_{11}, $C_{11}+C_{12}$, $C_{11}+C_{33}+2C_{13}$, C_{33}, and C_{44}, respectively, can be obtained. For each of the deformations, six different values for the strain parameter in the range $-0.02<\eta<0.02$ have been considered. When applying the D_2 and D_4 deformations to the solid, the unit cell remains hexagonal with the 12 original symmetry operators preserved. All other three deformations lower the symmetry: for D_1 and D_3 the system becomes monoclinic with only four operators, while in the D_5 deformation the symmetry is further reduced to triclinic with only two operators left.

An important point to consider is the positional relaxation of the atoms in the unit cell (inner contribution) caused by lattice strain. If that effect is neglected and the atomic fractional coordinates kept constant, then an upper limit (external contribution) is obtained for the value of each elastic constant. The results of this calculation are reported in the first column of Table VII. For each elastic constant, reoptimization of the inner positions (maintaining the appropriate symmetry constraints) has been performed only for the two end values of the η range ($-0.02<\eta<0.02$), where it is supposed to be most important. In the second and third columns of Table VII we report the inner contributions to elastic constants and the total calculated values. In the case of C_{44}, the total loss of symmetry results in the need for reoptimization of the position of all four unit-cell atoms. Taking into account the large computational effort needed to perform this task, only the external contribution has been evaluated for this constant.

To date, two full sets of measured elastic constants have been published for AlN.[11,17] In Tsubouchi's[17] work, elastic constants of AlN were evaluated from surface-acoustic-wave phase velocities on AlN single-crystal films grown on the basal plane of Al_2O_3. Recently, McNeil, Grimsditch, and French[11] have reported a measurement of all five elastic constants from Brillouin-scattering experiments on single crystals. Since experimental work

TABLE VII. Calculated (6-21G^* basis set) and experimental elastic constants (GPa) of AlN. Values in the three first columns (W calc.) refer to elastic constants calculated for the wurtzite structure. The external contribution to the elastic constants does not include the positional relaxation of the atoms caused by lattice strain, and the inner contribution is the correction for atomic relaxation. Values in the fourth (ZB) and fifth (W from ZB) columns are for the equivalent zinc-blende structure and those calculated for the wurtzite structure by using Martin's relations (Ref. 52), respectively.

	W calc. external	W calc. inner	W calc. total	ZB	W from ZB	Expt.	
C_{11}	537	−73	464	348	389	345[a]	411[d]
C_{12}	120	29	149	168	158	125[a]	149[d]
C_{13}	160	−44	116		138	120[a]	99[d]
C_{33}	512	−103	409		408	395[a], 394[b]	389[d]
C_{44}	128		128	135	101	118[a]	125[d]
B			231	228	228	202[a], 208[c]	237[d]

[a]Reference 17.
[b]Reference 53.
[c]Reference 44.
[d]Reference 11.

has only been performed at room temperature, no extrapolation to 0 K could be done, and comparison of these measured values with our calculated results is not straightforward.

The calculated values are somewhat larger than the experimental ones, which is the expected trend, since the temperature factor is not included in our calculations. As stated above, calculated elastic constants correspond to values extrapolated at 0 K and should be larger than the results from measurements at room temperature. C_{12} and C_{13} are affected by a larger numerical error because they are derived indirectly from linear combinations. This leads to a seemingly paradoxical result: the inner correction for the C_{12} constant is positive, while we expect negative values in all cases for this magnitude. Because the inner correction for C_{11} is more negative than that calculated for the linear combination $C_{11}+C_{12}$ used to obtain C_{12}, the total result gives a positive value.

Keeping in mind the discrepancy due to temperature factors, all calculated values are in good agreement with experimental results. Surprisingly the experimental value for C_{11} given by Tsubouchi[17] is lower than C_{33}, while in our calculations, in McNeil's[11] measurements, and in experimental values for related compounds with wurtzite structure [GaN and InN (Ref. 54)] the opposite trend is found.

The bulk modulus B for an hexagonal crystal can be evaluated from its elastic constants using the following expression:

$$B=\frac{C_{33}(C_{11}+C_{12})-2C_{13}^2}{C_{11}+C_{12}+2C_{33}-4C_{13}}\ .$$

The value obtained for the bulk modulus introducing the calculated elastic constants in this equation (see Table VII) is in good agreement with the value calculated with the method described above, and with the experimental value obtained from the elastic constants given by McNeil, Grimsditch, and French.[11]

An alternative way to obtain the elastic constants for a crystal with wurtzite structure consists in calculating these for the equivalent zinc-blende crystal and correlating its three elastic constants (C_{11}^c, C_{12}^c, and C_{44}^c) with the set of five elastic constants of the hexagonal phase (C_{11}^h, C_{12}^h, C_{13}^h, C_{33}^h, and C_{44}^h) using the symmetry descent procedure developed by Martin.[52] The advantage of this method is that it only requires the evaluation of three constants for the simpler cubic crystal, greatly reducing the computational effort.

The results obtained using this alternative method are summarized in Table VII. This procedure gives values which, although less accurate, agree reasonably well with the ones calculated explicitly for the wurtzite structure. At odds with the results of the direct method, the indirect evaluation of elastic constants gives $C_{11}^h<C_{33}^h$, leaving this ambiguity unsolved. These results indicate that the elastic constants of a compound with a wurtzite-type structure can be evaluated to a good approximation from the computationally less demanding calculation of the elastic constants for the equivalent cubic zinc-blende structure.

The elastic constants calculated for the zinc-blende structure of AlN agree well with the values $C_{11}=328$ GPa, $C_{12}=139$ GPa, and $C_{44}=133$ GPa calculated by Sherwin and Drummond[55] by applying the reverse of Martin's procedure to the experimental elastic constants of hexagonal AlN. From the calculated elastic constants for the cubic zinc-blende structure, a bulk modulus for the cubic phase of 228 GPa can be obtained from the relation $B=(C_{11}+2C_{12})/3$ that is valid for cubic crystals.

CONCLUDING REMARKS

We have evaluated several structural and physical properties for the hexagonal wurtzite-type phase of AlN using the periodic Hartree-Fock approach with both all-electron and pseudopotential basis sets. The calculated structural parameters are well reproduced with all four basis sets considered in this work. Inclusion of polarization functions in the basis set appreciably improves the calculated values of physical properties such as phonon vibration frequencies or elastic constants because it allows for a better description of electron relaxation throughout the unit cell. Since the bottleneck of Hartree-Fock calculations is the large number of bielectronic integrals to be computed, which is dictated mainly by the more diffuse basis functions, all-electron calculations can become paradoxically faster than pseudopotential ones, depending on the exponents of the basis functions employed for the description of the valence electrons.

The evaluation of physical properties such as elastic constants and phonon vibration frequencies for solids using the *ab initio* Hartree-Fock method yields results which are in fair agreement with measured values. This theoretical approach is thus expected to provide in the near future a powerful complement to experimental studies for the full characterization of technologically interesting materials with complex structures.

ACKNOWLEDGMENTS

The authors are grateful to C. Pisani, R. Dovesi, and C. Roetti for providing them with a copy of the CRYSTAL-92 code and for their helpful suggestions on its installation and use. The computing resources at the Centre de Supercomputació de Catalunya (CESCA) were generously made available through a CESCA grant. Financial support to this work was provided by DGYCIT through Grant No. PB92-0655.

[1]H. Schulz and K. H. Thiemann, Solid State Commun. **23**, 815 (1977).

[2]V. A. Fomichev, Fiz. Tverd. Tela (Leningrad) **10**, 763 (1968) [Sov. Phys. Solid State **10**, 597 (1968)].

[3]G. A. Slack, J. Phys. Chem. Solids **34**, 321 (1973).

[4]G. A. Slack, R. A. Tanzilli, R. O. Pohl, and J. W. Vandersande, J. Phys. Chem. Solids **48**, 641 (1987).

[5]O. Madelung, M. Schulz, and H. Weiss, in *Numerical Data and*

Functional Relationships in Science and Technology, edited by K.-H. Hellwege, Landolt-Börnstein, New Series, Group III, Vol. 17, Pt. a (Springer, Berlin, 1982).
[6]G. R. Kline and K. M. Lakin, Appl. Phys. Lett. **43**, 750 (1983).
[7]E. Gabe, Y. LePage, and S. L. Mair, Phys. Rev. B **24**, 5634 (1981).
[8]O. Brafman, G. Lengyel, S. S. Mitra, P. J. Gielisse, J. N. Plendl, and L. C. Mansur, Solid State Commun. **6**, 523 (1968).
[9]C. Carlone, K. M. Lakin, and H. R. Shanks, J. Appl. Phys. **55**, 4010 (1984).
[10]J. A. Sanjurjo, E. López-Cruz, P. Vogl, and M. Cardona, Phys. Rev. B **28**, 4579 (1983).
[11]L. E. McNeil, M. Grimsditch, and R. H. French, J. Am. Ceram. Soc. **76**, 1132 (1993).
[12]K. Hayashi, K. Itoh, S. Sawaki, and I. Akasaki, Solid State Commun. **77**, 115 (1991).
[13]P. Perlin, A. Polian, and T. Suski, Phys. Rev. B **47**, 2874 (1993).
[14]A. T. Collins, E. C. Lightowlers, and P. J. Dean, Phys. Rev. **158**, 833 (1967).
[15]R. V. Kasowski and F. S. Ohuchi, Phys. Rev. B **35**, 9311 (1987).
[16]M. Gautier, J. P. Duraud, and C. Le Gressus, Surf. Sci. **178**, 201 (1986).
[17]K. Tsubouchi, K. Sugai, and N. Mikoshiba, in *1981 Ultrasonics Symposia Proceedings,* edited by B. R. McAvoy (IEEE, New York, 1981), p. 375.
[18]B. Hejda and K. Hauptmanová, Phys. Status Solidi **36**, K95 (1969).
[19]S. Bloom, J. Phys. Chem. Solids **32**, 2027 (1971).
[20]A. Kobayashi, O. F. Sankey, S. M. Volz, and J. D. Dow, Phys. Rev. B **28**, 935 (1983).
[21]M.-Z. Huang and W. Y. Ching, J. Phys. Chem. Solids **46**, 977 (1985).
[22]W. Y. Ching and B. N. Harmon, Phys. Rev. B **34**, 5305 (1986).
[23]S. Loughin, R. H. French, W. Y. Ching, Y. N. Xu, and G. A. Slack, Appl. Phys. Lett. **63**, 1182 (1993).
[24]K. Miwa and A. Fukumoto, Phys. Rev. B **48**, 7897 (1993).
[25]P. E. Van Camp, V. E. Van Doren, and J. T. Devreese, Phys. Rev. B **44**, 9056 (1991).
[26]R. Pandey, A. Sutjianto, M. Seel, and J. E. Jaffe, J. Mater. Res. **8**, 1922 (1993).
[27]I. Gorczyca and N. E. Christensen, Physica B **185**, 410 (1993).
[28]N. E. Christensen and I. Gorczyca, Phys. Rev. B **47**, 4307 (1993).
[29]A. Muñoz and K. Kunc, Physica B **185**, 422 (1993).
[30]CRYSTAL-92: R. Dovesi, V. R. Saunders, and C. Roetti, University of Torino (Italy) and Landsbury Laboratory (U.K.), 1992.
[31]C. Pisani, R. Dovesi, and C. Roetti, *Hartree-Fock Ab-Initio Treatment of Crystalline Solids* (Springer-Verlag, Berlin, 1988), Vol. 48.
[32]R. Orlando, R. Dovesi, C. Roetti, and V. R. Saunders, J. Phys. Condens. Matter **2**, 7769 (1990).
[33]A. F. Wells, *Structural Inorganic Chemistry,* 5th ed. (Clarendon, Oxford, 1984), p. 538.
[34]*CRC Handbook of Chemistry and Physics,* 73rd ed., edited by D. R. Lide (Chemical Rubber Company, Boca Raton, 1992).
[35]F. S. Ohuchi, R. H. French, and R. V. Kasowskki, J. Appl. Phys. **62**, 2286 (1987).
[36]V. A. Fomichev, I. I. Zhukova, and I. K. Polushina, J. Phys. Chem. Solids **29**, 1025 (1968).
[37]E. Ruiz, S. Alvarez, and P. Alemany, Int. J. Quantum Chem. (to be published).
[38]N. N. Sirota, A. I. Olekhnovich, and N. M. Olekhnovich, Acta. Crystallogr. Sect. A **24**, 639 (1968).
[39]W. G. Fateley, F. R. Dollish, N. T. McDevitt, and F. F. Bentley, *Infrared and Raman Selection Rules for Molecular and Lattice Vibrations: The Correlation Method* (Wiley-Interscience, New York, 1972).
[40]D. L. Rousseau, R. P. Bauman, and S. P. S. Porto, J. Raman Spectrosc. **10**, 253 (1981).
[41]K.-M. Ho, C.-L. Fu, and B. N. Harmon, Phys. Rev. B **29**, 1574 (1984).
[42]K. Kunc and R. M. Martin, *Ab Initio Calculation of Phonon Spectra* (Plenum, New York, 1982), p. 65.
[43]K. Kunc and R. M. Martin, Phys. Rev. B **48**, 406 (1982).
[44]M. Ueno, A. Onodera, O. Shimomura, and K. Takemura, Phys. Rev. B **45**, 10 123 (1992).
[45]R. Dovesi, C. Roetti, C. Freyria-Fava, M. Prencipe, and V. R. Saunders, Chem. Phys. **156**, 11 (1991).
[46]M. Catti, R. Dovesi, A. Pavese, and V. R. Saunders, J. Phys. Condens. Matter **3**, 4151 (1991).
[47]M. Catti, A. Pavese, R. Dovesi, C. Roetti, and M. Causà, Phys. Rev. B **44**, 3509 (1991).
[48]J. A. Garber and A. V. Granato, Phys. Rev. B **11**, 3990 (1975).
[49]G. Liebfried and W. Ludwig, Solid State Phys. **12**, 275 (1961).
[50]D. Gerlich, S. L. Dole, and G. A. Slack, J. Phys. Chem. Solids **47**, 437 (1986).
[51]A. E. H. Love, *A Treatise on the Mathematical Theory of Elasticity* (Dover, New York, 1944).
[52]R. M. Martin, Phys. Rev. B **6**, 4546 (1972).
[53]W. J. Meng, J. A. Sell, T. A. Perry, and G. L. Eesley, J. Vac. Sci. Technol. A **11**, 1377 (1993).
[54]A. G. Every and A. K. McCurdy, in *Numerical Data and Functional Relationships in Science and Technology,* edited by O. Madelung and D. F. Nelson, Landolt-Börnstein, New Series, Group III, Vol. 29, Pt. a (Springer, Berlin, 1992).
[55]M. E. Sherwin and T. J. Drummond, J. Appl. Phys. **69**, 8423 (1991).